AMERICAN SOCIETY FOR MICROBIOLOGY | Applied and Environmental Microbiology®

GENETICS AND MOLECULAR BIOLOGY

Development of a CRISPR/Cas9 System for *Methylococcus capsulatus In Vivo* Gene Editing

Timothy Tapscott,[a] Michael T. Guarnieri,[a] Calvin A. Henard[a]

[a]National Bioenergy Center, National Renewable Energy Laboratory (NREL), Golden, Colorado, USA

ABSTRACT Methanotrophic bacteria play a crucial role in the Earth's biogeochemical cycle and have the potential to be employed in industrial biomanufacturing processes due to their capacity to use natural gas- and biogas-derived methane as a sole carbon and energy source. Advanced gene-editing systems have the potential to enable rapid, high-throughput methanotrophic genetics and biocatalyst development. To this end, we employed a series of broad-host-range expression plasmids to construct a conjugatable clustered regularly interspaced short palindromic repeats (CRISPR)/Cas9 gene-editing system in *Methylococcus capsulatus* (Bath). Heterologous coexpression of the *Streptococcus pyogenes* Cas9 endonuclease and a synthetic single guide RNA (gRNA) showed efficient Cas9 DNA targeting and double-stranded DNA (dsDNA) cleavage that resulted in cell death. We demonstrated effective *in vivo* editing of plasmid DNA using both Cas9 and Cas9^{D10A} nickase to convert green fluorescent protein (GFP)- to blue fluorescent protein (BFP)-expressing cells with 71% efficiency. Further, we successfully introduced a premature stop codon into the soluble methane monooxygenase (sMMO) hydroxylase component-encoding *mmoX* gene with the Cas9^{D10A} nickase, disrupting sMMO function. These data provide proof of concept for CRISPR/Cas9-mediated gene editing in *M. capsulatus*. Given the broad-host-range replicons and conjugation capability of these CRISPR/Cas9 tools, they have potential utility in other methanotrophs and a wide array of Gram-negative microorganisms.

IMPORTANCE In this study, we targeted the development and evaluation of broad-host-range CRISPR/Cas9 gene-editing tools in order to enhance the genetic-engineering capabilities of an industrially relevant methanotrophic biocatalyst. The CRISPR/Cas9 system developed in this study expands the genetic tools available to define molecular mechanisms in methanotrophic bacteria and has the potential to foster advances in the generation of novel biocatalysts to produce biofuels, platform chemicals, and high-value products from natural gas- and biogas-derived methane. Further, due to the broad-host-range applicability, these genetic tools may also enable innovative approaches to overcome the barriers associated with genetically engineering diverse, industrially promising nonmodel microorganisms.

KEYWORDS CRISPR/Cas9, *Methylococcus capsulatus*, gene editing, methane biocatalyst, methane monooxygenase, methanotroph

The clustered regularly interspaced short palindromic repeats (CRISPR)/CRISPR-associated protein 9 (Cas9) prokaryotic immune system from *Streptococcus pyogenes* has revolutionized genetic-engineering capabilities in a wide array of organisms. CRISPR/Cas9 gene editing is mediated by the programmable Cas9 endonuclease, which targets a genomic locus with high specificity and induces a double-stranded DNA (dsDNA) break (1–4). Target specificity is controlled by a coexpressed single guide RNA (gRNA) that contains a 20-base protospacer complementary to the target sequence, which is adjacent to a 5′-NGG-3′ protospacer-adjacent motif (PAM) site (2, 3).

Cas9-induced dsDNA breaks can result in repair via error-prone nonhomologous end

Citation Tapscott T, Guarnieri MT, Henard CA. 2019. Development of a CRISPR/Cas9 system for *Methylococcus capsulatus in vivo* gene editing. Appl Environ Microbiol 85:e00340-19. https://doi.org/10.1128/AEM.00340-19.

Editor Robert M. Kelly, North Carolina State University

Address correspondence to Michael T. Guarnieri, Michael.guarnieri@nrel.gov, or Calvin A. Henard, calvin.henard@nrel.gov.

T.T. and C.A.H. contributed equally to this work.

Received 8 February 2019
Accepted 22 March 2019
Accepted manuscript posted online 29 March 2019
Published 16 May 2019

joining (NHEJ) or high-fidelity homology-directed repair (HDR) (5). Although a subset of bacteria contain Ku- and DNA ligase-catalyzed NHEJ systems, most rely on RecA/RecBCD-dependent HDR to repair Cas9-induced dsDNA breaks (5, 6). In bacteria in which dsDNA breaks have been reported to be lethal, the Cas9^{D10A} nickase has been successfully employed for CRISPR-based gene editing (7–9). This variant contains a disabled RuvC1 nuclease domain that can induce single-stranded DNA (ssDNA) nicks in order to induce single-nick-assisted HDR (3, 7–9). In some microbes tested, Cas9^{D10A} mediated higher gene editing efficiencies than wild-type Cas9 (7–9). Combined, these CRISPR/Cas9 tools can enable robust multiplex and high-throughput gene-editing strategies (10–12) and may fast track the development of nonmodel microorganisms with limited genetic tractability for industrial applications.

Methanotrophic bacteria are key players in Earth's biogeochemical carbon cycle and are of increasing industrial interest for their capacity to utilize methane as a sole carbon and energy source (13). The model gammaproteobacterial methanotroph *Methylococcus capsulatus* has been extensively studied for decades and is currently used for the industrial production of single-cell protein. Broad-host-range replicative plasmids containing RP4/RK2, RSF1010, and pBBR1 replicons are functional in *M. capsulatus* and have enabled the development of promoter-probe vectors and heterologous gene expression in the organism (14, 15). Further, chromosomal insertions and unmarked genetic mutations using allelic-exchange vectors and sucrose or p-chlorophenylalanine counterselection have been reported (15–19). These tools have served as a basis for the recent expansion of the methanotroph genetic toolbox that has enabled several proteobacterial methanotrophs to be engineered to convert methane-rich natural gas and aerobic-digestion-derived biogas into high-value products (20–25). Notably, these tools also lay the foundation for the development of advanced CRISPR genome-editing systems that facilitate multiplex or high-throughput gene-editing strategies. The development of advanced genome-editing tools offers a means to enable rapid evaluation of fundamental methanotrophic governing mechanisms while expanding metabolic engineering capabilities in these hosts for methane sequestration, bioremediation, and biomanufacturing.

In this study, we developed broad-host-range CRISPR/Cas9 gene-editing tools and evaluated their efficacy in the methanotroph *M. capsulatus*. Using the CRISPR/Cas9 system, we demonstrated editing of methanotroph-harbored plasmid DNA by introducing *in vivo* point mutations in a gene encoding green fluorescent protein (GFP) to generate a blue fluorescent protein (BFP) variant. Further, we successfully achieved chromosomal editing by generating a soluble methane monooxygenase (sMMO) mutant strain via the introduction of a premature stop codon in the *mmoX* open reading frame using the Cas9^{D10A} nickase. The CRISPR/Cas9 tools developed here will facilitate the development of advanced methanotrophic biocatalysts and have potential utility in an array of nonmodel, industrially promising bacteria.

RESULTS AND DISCUSSION

Development of a broad-host-range CRISPR/Cas9 gene-editing system. We employed the superfolder GFP (26) reporter to evaluate the functionality and strength of heterologous and native *M. capsulatus* promoters to be used for expression of Cas9 nuclease and gRNA components. We tested whether pCAH01, an RK2-based broad-host-range expression plasmid that contains the inducible tetracycline promoter/operator (P_{tetA}), previously demonstrated to function in the related gammaproteobacterial methanotroph *Methylomicrobium buryatense* 5GB1 (21, 23), was also functional in *M. capsulatus*. The P_{tetA} promoter exhibited strong inducible activation in *M. capsulatus*, as indicated by an ~10-fold increase of GFP fluorescence in pCAH01::GFP-harboring cells after exposure to the anhydrotetracycline (aTc) inducer (Fig. 1A). Based on the ability to temporally control gene expression, Cas9- and the Cas9^{D10A} nickase variant-encoding genes were cloned downstream of P_{tetA} in pCAH01Sp^R to generate pCas9 (Fig. 2A) and pCas9^{D10A}, respectively (see Fig. S1A in the supplemental material).

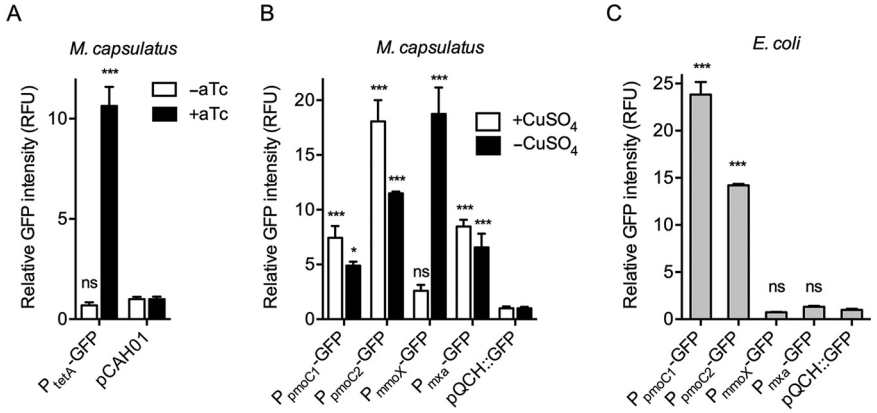

FIG 1 Promoter activity in *M. capsulatus*. (A) GFP fluorescence in *M. capsulatus* expressing GFP from the tetracycline promoter/operator (P_{tetA}) in pCAH01::GFP. Where indicated, GFP was induced by plating on NMS agar supplemented with 500 ng/ml aTc for 72 h. The empty pCAH01 plasmid was used as a negative control. (B) GFP fluorescence in *M. capsulatus* with GFP expression controlled by the indicated gene promoters in pQCH::GFP. Fluorescence intensity was measured from cells grown on NMS agar with or without 5 μM $CuSO_4$ for 72 h. (C) GFP fluorescence in *E. coli* expressing GFP from the indicated promoters in pQCH::GFP. Fluorescence intensity was measured from cells grown to an OD_{600} of 0.5 in LB liquid medium. In panels B and C, the promoterless pQCH::GFP plasmid was used as a negative control. The data represent the fluorescence intensity normalized to OD_{600} and are depicted as mean RFU and standard deviations (SD) from 3 independent replicates. ***, $P < 0.001$; *, $P < 0.05$; ns, not significant.

Next, we evaluated the activity of *M. capsulatus* promoters to select a suitable promoter to drive constitutive gRNA expression. Promoters from the gamma subunit of particulate methane monooxygenase 1 (P_{pmoC1}), particulate methane monooxygenase 2 (P_{pmoC2}), the sMMO hydroxylase component *mmoX* (P_{mmoX}), and methanol dehydrogenase *mxaF* (P_{mxa}) genes were cloned upstream of a GFP coding sequence in the RSF1010-derived vector pQCH (see Fig. S1B), and promoter activity was assessed via fluorescence. As previously demonstrated via transcriptomic studies (19, 27, 28), P_{pmoC1}, P_{pmoC2}, and P_{mxa} were highly active in *M. capsulatus*, driving significant GFP transcription under both copper-replete and copper-depleted conditions (Fig. 1B). As expected, we detected limited P_{mmoX} promoter activity under copper-replete growth conditions; however, an ~7.5-fold increase in GFP expression was observed when cells were grown under copper-depleted conditions (Fig. 1B) (19, 27, 28). Notably, the copper switch-regulated P_{mmoX} promoter may be employed for the inducible expression of heterologous genes in *M. capsulatus*. Both P_{pmoC1} and P_{pmoC2} were functional in *Escherichia coli*, but, interestingly, P_{mxa} and P_{mmoX} promoter activity was not detected in the organism (Fig. 1C), presumably due to the absence of required regulatory factors unique to *M. capsulatus* (15). Based on these results, we chose the P_{mxa} promoter to express the gRNA due to the undetectable levels of GFP expression from this promoter in *E. coli* in order to avoid gRNA expression during cloning or conjugation procedures. A schematic of the broad-host-range plasmid pBBR1 containing a P_{mxa}-expressing gRNA and a 1-kb DNA repair template (pgRNA) is depicted in Fig. 2B.

Initial experiments evaluating Cas9 or $Cas9^{D10A}$ expression in *M. capsulatus* indicated that nuclease expression did not affect bacterial growth in the absence of gRNA expression (Fig. 2D). Next, Cas9 or $Cas9^{D10A}$ was coexpressed with an *mmoX*-targeting gRNA to evaluate nuclease targeting and activity using cell viability as a phenotypic readout. Transformants coexpressing Cas9 and pgRNA-*mmoX* exhibited ~99% cell death compared to cells expressing Cas9 without a gRNA (Fig. 2E). The surviving ~1% represent the background of the system and may serve as a putative limiting factor for gene-editing efficiency (29). Conversely, DNA digestion by $Cas9^{D10A}$ did not result in cell death (Fig. 2E) and, assuming $Cas9^{D10A}$ is functional under these experimental conditions, indicates that dsDNA breaks have a high degree of lethality while ssDNA nicks are more efficiently repaired by native *M. capsulatus* systems.

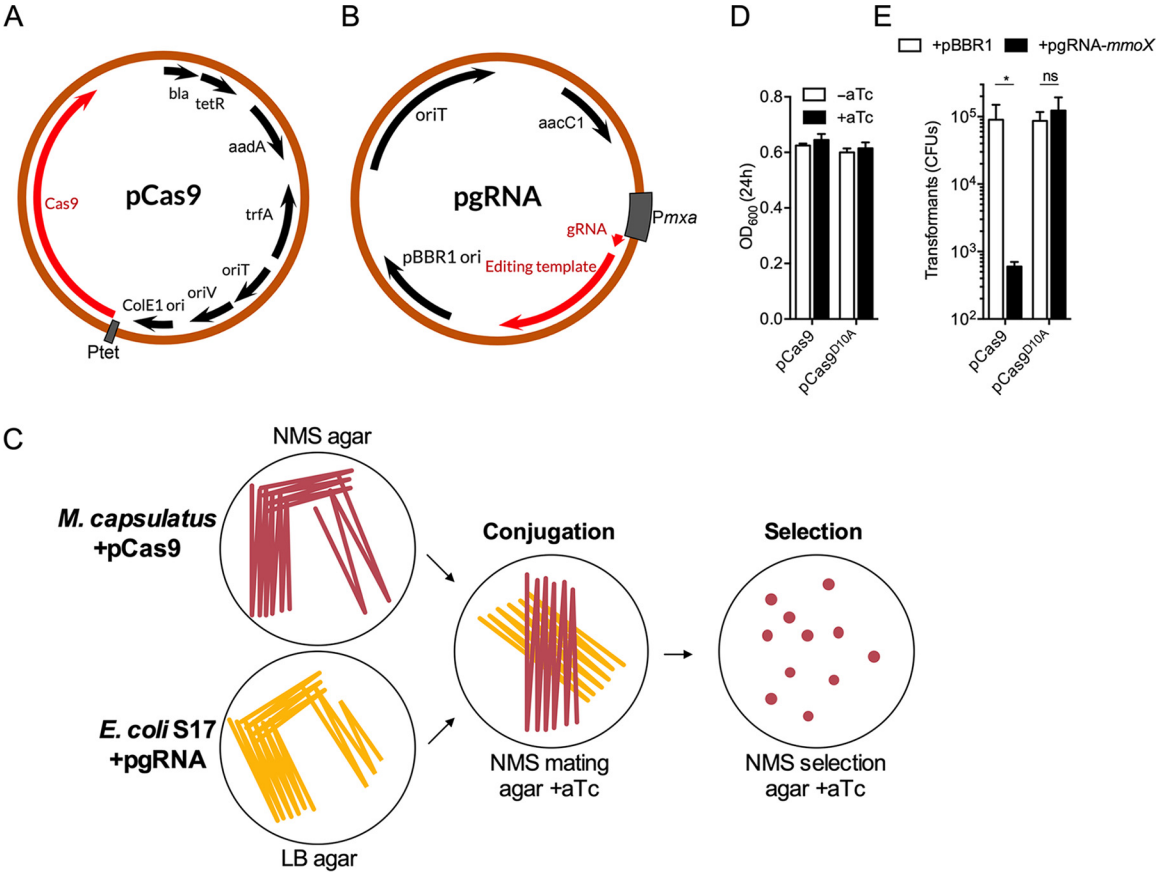

FIG 2 Broad-host-range CRISPR/Cas9 gene-editing system. (A) Plasmid map of pCAH01Sp^R::Cas9 (pCas9). Inducible expression of Cas9 is driven from the tetracycline promoter/operator (P_{tetA}). (B) Plasmid map of pBBR1-gRNA (pgRNA) containing a 1-kb DNA repair template. Expression of the gRNA is driven from the *M. capsulatus mxaF* promoter (P_{mxa}). (C) Experimental design schematic of the CRISPR/Cas9 gene-editing system. *M. capsulatus* harboring pCas9 was conjugated with *E. coli* S17 harboring pgRNA on NMS mating agar supplemented with 500 ng/ml aTc. After 48 h of conjugation, the biomass was spread onto NMS selection agar containing 500 ng/ml aTc, gentamicin, and spectinomycin until colonies appeared. (D) OD_{600} of bacterial cultures 24 h postinoculation with (+aTc) or without (−aTc) Cas9 or Cas9^{D10A} induction. The cultures were inoculated at an OD_{600} of 0.1. (E) CFU of Cas9- or Cas9^{D10A}-expressing *M. capsulatus* after conjugation with pgRNA-*mmoX*. Empty pBBR1 plasmid was used as a negative control. The data are depicted as mean CFU and SD from 3 independent replicates. *, $P < 0.05$; ns, not significant.

***In vivo* plasmid editing.** To evaluate CRISPR/Cas9 gene editing in *M. capsulatus*, we employed a screening assay with a direct fluorescent readout that shifts the emission and excitation of GFP to that of BFP following targeted gene editing (30). We constructed a vector (pgRNA-GFP^{BFP}) with a *gfp*-targeting gRNA and a 1-kb DNA repair template containing the GFP point mutations 194C→G, 196T→C, and 201T→G, which introduces the missense codon substitutions T64S and Y65H to convert GFP to BFP while concurrently abolishing the Cas9 PAM site (Fig. 3A; see Fig. S2 in the supplemental material). No detectable BFP fluorescence, only GFP fluorescence, was observed in cells expressing pgRNA-GFP^{BFP} and GFP, demonstrating that the native homologous-recombination machinery did not integrate the DNA repair template into the *gfp* locus in the absence of Cas9 and that BFP is not expressed from the pgRNA-GFP^{BFP} repair template (Fig. 3B). Positive transformants coexpressing Cas9, pgRNA-GFP^{BFP}, and GFP were analyzed for BFP fluorescence to determine editing efficiency. In the absence of Cas9 induction, we observed ~5% BFP-positive transformants after selection (Fig. 3B), indicating that leaky Cas9 expression from P_{tetA} is sufficient for gene editing. The induction of Cas9 during the conjugal transfer of pgRNA-GFP^{BFP} significantly increased plasmid DNA-editing efficiency, with 71% of the transformants originally encoding GFP now expressing BFP (Fig. 3B). Fluorescence microscopy of isolated BFP-expressing colonies showed that all the cells uniformly expressed BFP, with no GFP-expressing cells

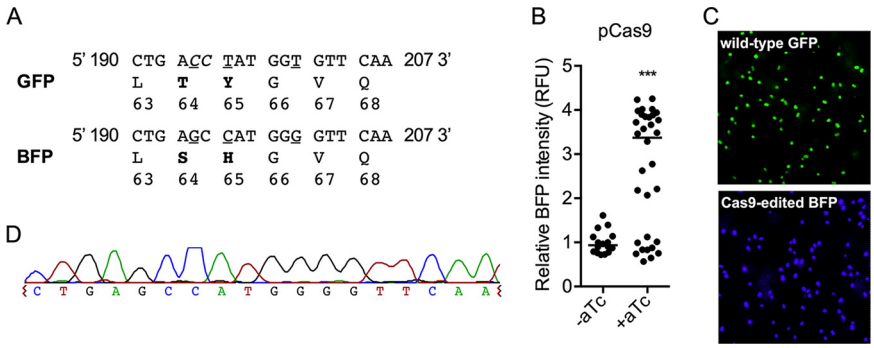

FIG 3 CRISPR/Cas9-targeted editing of plasmid DNA converting GFP to BFP. (A) Amino acid (boldface) and nucleotide (underlined) substitutions required to convert GFP to BFP with the Cas9 PAM site (italicized). (B) BFP intensity of Cas9-expressing *M. capsulatus* after conjugation with pgRNA-GFP^{BFP}. Where indicated, Cas9 was induced by plating on NMS agar supplemented with 500 ng/ml aTc during mating and selection. Each data point represents the fluorescence intensity of a unique colony as RFU normalized to the OD_{600}. The horizontal line represents the median fluorescence intensity. (C) Representative fluorescence micrograph of GFP-expressing and Cas9-edited BFP-expressing *M. capsulatus*. (D) Representative sequencing chromatogram of a Cas9-edited pQCH::P_{pmoC1}-BFP locus. ***, $P < 0.001$.

observed in the colony population (Fig. 3C). Sequence analysis of the fluorescent-protein-encoding loci from transformants identified as BFP positive confirmed the incorporation of the p.T64S and p.Y65H GFP-to-BFP mutations (Fig. 3D).

Similar to the experimental design with Cas9 described above, we tested whether the Cas9^{D10A} nickase could also be utilized for targeted DNA editing. In the absence of Cas9^{D10A} induction, no BFP fluorescence was detected in pgRNA-GFP^{BFP}-expressing transformants (Fig. 4A). However, when Cas9^{D10A} and pgRNA-GFP^{BFP} were coexpressed, we found that 71% of the transformants exhibited BFP fluorescence at varying intensities (Fig. 4A). Intriguingly, many BFP-expressing transformants were also positive for GFP fluorescence, with the degree of BFP fluorescence intensity positively correlated with a decrease in GFP fluorescence intensity (Fig. 4B). Fluorescence microscopy showed that transformant colonies consisted of both GFP- and BFP-expressing cells (Fig. 4C), presumably due to the expansion of plasmid copies that either were not cleaved by Cas9^{D10A} or were repaired after cleavage without incorporation of the homologous DNA repair template.

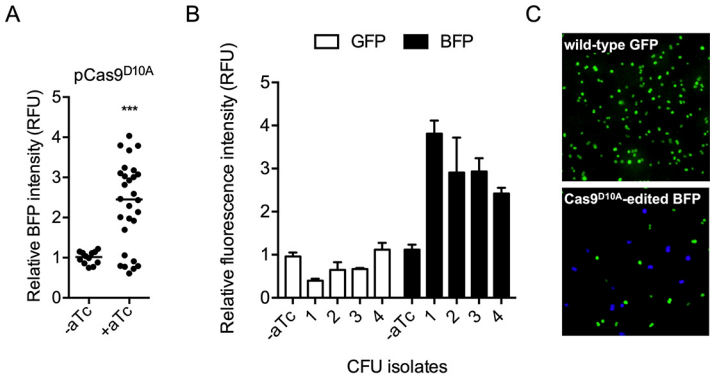

FIG 4 CRISPR/Cas9^{D10A} nickase-targeted editing of plasmid DNA converting GFP to BFP. (A) BFP fluorescence in Cas9^{D10A}-expressing *M. capsulatus* after conjugation with pgRNA-GFP^{BFP}. Where indicated, Cas9^{D10A} was induced by plating on NMS agar supplemented with 500 ng/ml aTc during mating and selection. Each data point represents the fluorescence intensity of a unique colony as RFU normalized to the OD_{600}. The horizontal line represents the median fluorescence intensity. (B) BFP and GFP fluorescence in representative transformants coexpressing Cas9^{D10A} and pgRNA-GFP^{BFP}. The data represent mean RFU and SD from 3 independent replicates. (C) Representative fluorescence micrograph of Cas9^{D10A}-edited BFP-expressing *M. capsulatus* cells. ***, $P < 0.001$.

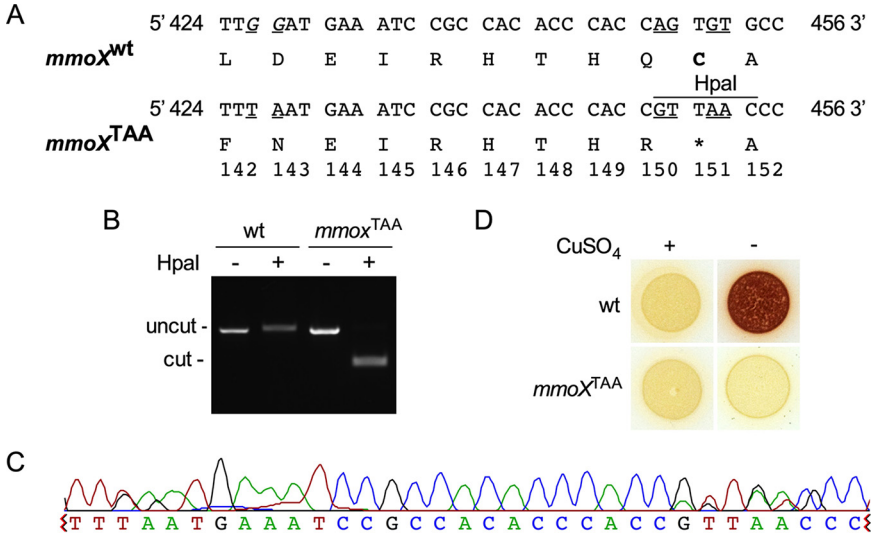

FIG 5 CRISPR/Cas9^{D10A}-mediated editing of the *M. capsulatus* sMMO hydroxylase *mmoX* chromosomal locus. (A) Nonsense codon (boldface) and nucleotide (underlined) substitutions for generation of the *mmoX* p.C151X (*mmoX*^{TAA}) mutation with the Cas9 PAM site shown (italicized). wt, wild type. (B) Representative agarose gel showing HpaI-digested *mmoX* PCR products from the wild type or a positive *mmoX*^{TAA} transconjugant. (C) Representative sequencing chromatogram of a Cas9^{D10A}-edited *mmoX*^{TAA} locus. (D) Wild-type and *mmoX*^{TAA} biomass on NMS agar with or without 5 μM $CuSO_4$. The activity of sMMO was assessed by naphthalene and *o*-dianisidine colorimetric assay. Positive sMMO activity is indicated by development of red coloration.

***In vivo* genome editing.** We next evaluated Cas9- and Cas9^{D10A}-mediated chromosomal editing by targeting the *mmoX* gene encoding the sMMO hydroxylase component. We constructed a vector that harbored an *mmoX*-targeting gRNA and a DNA repair template containing an HpaI endonuclease restriction site, GTTAAC, which concurrently introduces a nonsense *mmoX* C151X (*mmoX*^{TAA}) mutation (pgRNA-*mmoX*^{TAA}) (Fig. 5A; see Fig. S3 in the supplemental material). Transformants coexpressing pgRNA-*mmoX*^{TAA} and Cas9 or Cas9^{D10A} were screened by colony PCR and subsequent digestion with HpaI endonuclease. We were unable to isolate an *mmoX*^{TAA} transformant in Cas9- and pgRNA-*mmoX*^{TAA}-expressing tranformants. In contrast, we identified the targeted *mmoX*^{TAA} edit in 2% (5/250) of the Cas9^{D10A} nickase- and pgRNA-*mmoX*^{TAA}-expressing transformants, as verified by HpaI digestion (Fig. 5B). Incorporation of the *mmoX*^{TAA} nonsense mutation into the chromosome was also verified by sequence analysis (Fig. 5C). Further, the colorimetric sMMO activity assay demonstrated that the *mmoX*^{TAA} strain was unable to convert naphthalene to naphthol after copper-depleted growth, confirming disruption of sMMO functionality (Fig. 5D).

Inducing single-nick-assisted HDR by the Cas9^{D10A} nickase has been employed in other microbes when wild-type Cas9-based editing has been unsuccessful (7–9). Previous studies have demonstrated that single-nick-assisted HDR undergoes repair via an independent mechanism with higher fidelity than dsDNA break-induced repair (31). Our data indicate that the Cas9^{D10A}-mediated nick induces higher chromosome recombination efficiency than a wild-type Cas9 dsDNA break, leading to increased numbers of transformants and enhanced *mmoX* locus-editing efficiency (Fig. 2D and 5). Intriguingly, contrary to the differential observed for chromosomal editing, plasmid-editing efficiencies were identical whether Cas9 or Cas9^{D10A} was utilized. Future studies are thus needed to understand the differences in plasmid- and chromosome-editing efficiencies observed during the course of these investigations. Notably, successful incorporation of exogenous DNA into plasmid or genomic DNA by *M. capsulatus* was achieved via native recombination machinery. Evaluating the efficacy of heterologous recombinases, such as those employed in lambda red recombineering, may offer a potential means to enhance Cas9-mediated editing while also decreasing repair template size requirements (32, 33).

TABLE 1 Strains and plasmids

Name	Genotype or description	Source
Strains		
Methylococcus capsulatus Bath	Wild type	ATCC 33009
E. coli Zymo 10B	F$^-$ *mcrA* Δ(*mrr-hsdRMS-mcrBC*) Φ80*lacZ*ΔM15 Δ*lacX74 recA1 endA1 araD139* Δ(*ara leu*) 7697 *galU galK rpsL nupG* λ$^-$	Zymo Research
E. coli S17-1	Tp^r Sm^r *recA thi pro hsd*(r$^-$ m$^+$)RP4-2-Tc::Mu::Km Tn*7*	ATCC 47055
Plasmids		
pCAH01	P_{tetA}*bla tetR* CoE1 *ori* F1 *oriV oriT trfA ahp*	21
pCAH01Sp^R	*ahp CDS* exchanged with *aadA CDS*	This study
pCAH01::GFP	GFP cloned downstream of P_{tetA}	21
pCAH01Sp^R::Cas9	Cas9 cloned downstream of P_{tetA}	This study
pAWP78	Source of *ahp* locus used to generate pQCH	25
RSF1010	*oriV oriT mobABC repABC sul2 strAB*	44
pQCH	RSF1010Δ[7.626-2.200 kb] *ahp*	This study
pQCH::GFP	pQCH with promoterless superfolder GFP	This study
pQCH::P_{mmoX}-GFP	P_{mmoX} cloned upstream of GFP in pQCH::GFP	This study
pQCH::P_{mxa}-GFP	P_{mxa} cloned upstream of GFP in pQCH::GFP	This study
pQCH::P_{pmoC1}-GFP	P_{pmoC1} cloned upstream of GFP in pQCH::GFP	This study
pQCH::P_{pmoC2}-GFP	P_{pmoC2} cloned upstream of GFP in pQCH::GFP	This study
pQCH::P_{pmoC1}-BFP	P_{pmoC1}-BFP cloned from P_{pmoC1}-GFP	This study
pBBR1MCS-5	pBBR *oriT aacC1*	45
pBBR1-GFP	P_{mxa}-gRNA-GFP cloned into pBBR1	This study
pBBR1-GFP^{BFP}	P_{mxa}-gRNA-GFP^{BFP} cloned into pBBR1	This study
pBBR1-*mmoX*	P_{mxa}-gRNA-*mmoX* cloned into pBBR1	This study
pBBR1-*mmoX*^{TAA}	P_{mxa}-gRNA-*mmoX*^{TAA} cloned into pBBR1	This study

Conclusions. Rational metabolic-engineering pursuits in methanotrophic bacteria require several metabolic mutations in order to enhance metabolic flux, end products, stress tolerances, and substrate utilization for the improved production of bio-based products (20). The tools developed here may enable CRISPR-based multiplex gene knockout strategies that can accelerate this time- and labor-intensive process. Further, CRISPR-based gene editing, together with high-throughput oligonucleotide synthesis, presents a path to genetic-library construction targeting rate-limiting metabolic enzymes to isolate strains with enhanced or altered characteristics (10, 12). The ability to utilize Cas9 for DNA targeting makes it possible to also leverage the suite of available Cas9 variants (e.g., dCas9) (34–41) for transcriptional control, development of novel regulatory circuits, or optimization of CRISPR/Cas editing efficiency to enable advanced synthetic biology applications in methanotrophic bacteria.

In this study, we developed dual-plasmid, broad-host-range CRISPR/Cas9 tools and demonstrated targeted plasmid and chromosomal DNA editing with Cas9 and Cas9^{D10A} in the methanotroph *M. capsulatus*. This genetic system represents an advance in methanotroph molecular microbiology via expansion of the genetic toolbox. These advanced genetic tools may facilitate innovative strain engineering strategies that enable the development of methanotrophic biocatalysts for the production of biofuels, platform chemicals, and high-value products from methane. Further, novel molecular mechanisms underlying methanotroph biology can be probed with the addition of CRISPR/Cas9 to the methanotroph genetic toolbox. The replicons utilized in the CRISPR/Cas9 system developed here are recognized by phylogenetically diverse bacteria; thus, they have the potential to facilitate facile genetic querying and innovative strain-engineering strategies for the development of industrial biocatalysts in an array of nonmodel microbes.

MATERIALS AND METHODS

Bacterial strains and cultivation conditions. The strains used in this study are described in Table 1. *Methylococcus capsulatus* (Bath) was cultured on modified nitrate mineral salts (NMS) agar supplemented with 5 μM $CuSO_4$ (the formulation is shown in Table S1 in the supplemental material), unless otherwise indicated, at 37°C inside stainless-steel gas chambers (Schuett-biotec GmbH) containing 20% (vol/vol) methane in air (42). The NMS agar was supplemented with 100 μg/ml kanamycin, 100 μg/ml spectinomycin, and/or 30 μg/ml gentamicin for selection and cultivation of the respective *M. capsulatus*

TABLE 2 Primers

Purpose	Primer name[a]	Sequence[b]
Insert *aadA* into pCAH01	CAH520 *aadA* F	cagtgttacaaccaattaaccaattctgatTTATTTGCCGACTACCTTG
	CAH521 *aadA* R	cttacataaacagtaatacaaggggtgttaATGGCTTGTTATGACTGTTTTTTTG
	CAH522 pCAH01 F	TAACACCCCTTGTATTACTG
	CAH519 pCAH01 R	ATCAGAATTGGTTAATTGGTTG
Clone Cas9 into pCAH01	TT16 Cas9 F	cactccctatcagtgatagagaaaagtgaaATGGATAAGAAATACTCAATAGGC
	CAH537 Cas9 R	cttcacaggtcaagcttTTTTAGGAGGCAAAAATGGATAAG
	CAH152 pCAH01 F	AAGCTTGACCTGTGAAGTG
	CAH149 pCAH01 R	TTCACTTTTCTCTATCACTGATAG
Construct Cas9^{D10A}	TT143 Cas9^{D10A} F	GAAATACTCAATAGGCTTAGCCATCGGCACAAATAGCGTCG
	TT144 Cas9^{D10A} R	CGACGCTATTTGTGCCGATGGCTAAGCCTATTGAGTATTTC
Construct pQCH	CAH1032 *ahp* F	ttatattcaatggcttatttGCTCGGGACGCACGGCGC
	CAH1033 *ahp* R	cggaacatgcctcatgtggcGCGTGATCTGATCCTTCAACTCAGCAAAAGTTCGATTTAT
	CAH1034 RSF1010 F	GCCACATGAGGCATGTTCCG
	CAH1031 RSF1010 R	AAATAAGCCATTGAATATAAAAGATAAAAATGTC
Construct pQCH::GFP	CAH1044 pQCH F	CATACAGTCTATCGCTTAGCG
	CAH1037 pQCH R	TATTGCAAGGACGCGGAAC
	CAH1045 GFP F	ATGAGCAAAGGAGAAGAAC
Amplify pQCH::GFP parts	CAH1040 GFP F	gaggaaacaagtaATGAGCAAAGGAGAAGAAC
	CAH1041 GFP R	ttatttgatgcctTTATTTGTAGAGCTCATCC
	CAH1042 rrnBT1T2 F	gctctacaaataaAGGCATCAAATAAAACGAAAGGC
	CAH1043 rrnBT1T2 R	tttccgctaagcgatagactgtatgCATCCGTCAGGATGGCCTTC
Clone promoters into pQCH::GFP	CAH1046 P_{mxa} F	aggcatgttccgcgtccttgcaataGAGGTTCAGGCGAAACCG
	CAH1047 P_{mxa} R	ctcctttgctcatGTGTCTCCTCCAAGAATGATTG
	CAH1048 P_{pmoC1} F	aggcatgttccgcgtccttgcaataAACGTCACGATGGGTGTTC
	CAH1049 P_{pmoC1} R	ctcctttgctcatTGTTTGTTCCTCCTAAAGTGATG
	CAH1050 P_{pmoC2} F	aggcatgttccgcgtccttgcaataCCCTCGTGTCCGGCGTAC
	CAH1051 P_{pmoC2} R	ctcctttgctcatTTTTACCTCCAACTGTTATATCGATGTGAACAC
	CAH1038 P_{mmoX} F	aggcatgttccgcgtccttgcaataTCCGCAGTGGTCGGATCG
	CAH1039 P_{mmoX} R	ctcctttgctcatTACTTGTTTCCTCCGTAACACATTCTATG
Construct pgRNA-GFP and pgRNA-*mmoX*	TT254 P_{mxa} gRNA F	tccaattcgccctatagtgaGAGGTTCAGGCGAAACCG
	TT272 gRNA only R	gcaatagacataagcggctaGGATCAGATCACGCATCTTC
	TT256 pBBR1 F	TAGCCGCTTATGTCTATTGCTG
	TT253 pBBR1 R	TCACTATAGGGCGAATTGGAG
Construct GFP^{BFP} editing template	TT207 GFP F	atctgatccttcggaccgacggattGGACCGACGGATTTTATG
	TT208 BFP R	cattgaaccccatggcTCAGAGTAGTGACAAGTGTTG
	TT209 BFP F	ctactctgagccatgggGTTCAATGCTTTTCCCGTT
	TT255 GFP R	gcaatagacataagcggctaTGCCATGTGTAATCCCAG
Check GFP/BFP editing locus	TT288 GFP check F	TCCGCGTCCTTGCAATAAAC
	TT289 GFP check R	CCGCTAAGCGATAGACTGTATG
	TT271 GFP seq R	GTACATAACCTTCGGGCATG
Check *mmoX* editing locus	TT290 *mmoX* check F	CCAGTACGTCACCGTTATG
	TT291 *mmoX* check R	AGATCTTGCCGTAGTGGTC
	TT292 *mmox* seq F	CTGGAAGTGGGCGAATAC

[a]F, forward; R, reverse.
[b]Lowercase indicates homologous sequence for Gibson assembly.

strains. *E. coli* strains were cultured on lysogeny broth (LB) agar or in LB liquid medium at 37°C at 200 rpm. LB liquid medium was supplemented with 50 μg/ml kanamycin, 50 μg/ml spectinomycin, 10 μg/ml gentamicin, and/or 100 μg/ml ampicillin for selection and cultivation of the respective *E. coli* strains. Broad-host-range plasmids were transferred to *M. capsulatus* via biparental mating using *E. coli* S17-1 cells on NMS mating agar (the formulation is shown in Table S1), as described previously (25). Prior to conjugation, *M. capsulatus* biomass harboring pCas9 or pCas9^{D10A} was spread on NMS mating medium supplemented with 500 ng/ml aTc and incubated at 37°C inside stainless-steel gas chambers (Schuett-biotec GmbH) containing 20% (vol/vol) methane (99.97% purity) in air for 24 h. A schematic of the experimental design for using the CRISPR/Cas9 system in *M. capsulatus* is shown in Fig. 2C.

To evaluate promoter activity, *M. capsulatus* harboring GFP reporter plasmids was spread onto NMS agar supplemented with 0 μM or 5 μM $CuSO_4$. GFP expression from the tetracycline promoter/operator

(P_{tetA}) in pCAH01 was induced by plating on NMS agar supplemented with 500 ng/ml aTc. Strains were incubated at 37°C inside stainless-steel gas chambers (Schuett-biotec GmbH) in 20% (vol/vol) methane in air for 72 h, and the GFP fluorescence intensity was quantified as described below. Promoter activity was determined in *E. coli* subcultured 1/100 in LB liquid medium and incubated for ~3 h to an optical density at 600 nm (OD_{600}) of 0.5 at 37°C at 200 rpm. A 200-μl volume of *E. coli* cell suspension was transferred to a 96-well plate for quantification of the GFP fluorescence intensity as described below.

Cloning and genetic manipulation. The plasmids used in this study are described in Table 1. The primers and synthetic DNA fragments used in this study were synthesized by Integrated DNA Technologies, Inc. (IDT), and are described in Table 2 and Table S2 in the supplemental material, respectively. Plasmids and DNA inserts were amplified using Q5 High-Fidelity 2× Master Mix (NEB), assembled using Gibson NEBuilder HiFi DNA assembly (New England Biolabs), and transformed into Mix and Go competent *E. coli* strain Zymo 10B (Zymo Research), according to the manufacturers' instructions. Genetic constructs were verified by Sanger sequencing (Genewiz). The Cas9 open reading frame was amplified, using primers TT16 and CAH537 (Table 2), from Addgene plasmid no. 42876 (29) and cloned into pCAH01Sp^R via Gibson assembly. The $Cas9^{D10A}$ nickase variant was generated by site-directed mutagenesis with primers TT143 and TT144 (Table 2) using the QuikChange primer design program and protocol (Agilent). Single gRNAs containing a 20-mer adjacent to the PAM site on the target DNA and editing cassettes were synthesized by IDT (see Table S2) and cloned into the pBBR1MCS-5 vector via Gibson assembly. pQCH was constructed by replacing a 3,312-bp region of RSF1010 containing the *sulfR*, *smrA*, and *smrB* genes with the *kan2* locus from pAWP78 (25). To evaluate promoter activity, native *M. capsulatus* promoters were cloned upstream of the superfolder green fluorescent protein-encoding gene (26) into pQCH.

GFP and BFP expression quantification. To evaluate Cas9- and $Cas9^{D10A}$-mediated plasmid editing, fluorescence intensity was measured in a Fluostar Omega microplate reader (BMG Labtech) at an excitation wavelength (λ_{ex}) of 485 nm and an emission wavelength (λ_{em}) of 520 nm (GFP) or a λ_{ex} of 355 nm and a λ_{em} of 460 nm (BFP). For GFP-to-BFP gene-editing experiments, the data represent relative fluorescence units (RFU) of the measured BFP intensity relative to pQCH::P_{pmoC1}-GFP control intensity normalized to the cell density.

Verification of mutations by colony PCR and HpaI digestion. To evaluate Cas9- and $Cas9^{D10A}$-mediated genomic editing of the *mmoX* locus, colony PCR was performed with primers TT290 and TT291 (Table 2) using *Taq* 2× Master Mix (NEB) according to the manufacturer's instructions. The PCR mixture was used directly as the template for HpaI endonuclease (NEB) digestion, and the edited strains were identified by positive DNA digestion visualized by DNA electrophoresis. Targeted editing of the *mmoX* locus in positive transformants was verified by sequence analysis.

Colorimetric sMMO assay. *M. capsulatus* sMMO activity was tested with a colorimetric assay as previously described (43). Briefly, ~1e6 cells were spotted onto NMS agar with or without 5 μM $CuSO_4$ and cultured at 37°C. After 96 h of growth, ~300 to 400 mg naphthalene (Sigma-Aldrich) crystals was placed into the petri dish lid and incubated with the bacteria for 1 h at 37°C to allow conversion of naphthalene to naphthol. After incubation, 20 μl of freshly prepared 5-mg/ml *o*-dianisidine (Sigma-Aldrich), which turns purple in the presence of naphthol, was added directly to the *M. capsulatus* biomass. Color development was allowed to occur for 15 min at 37°C.

Statistical analysis. Statistical analysis of data was performed and graphical representations were created using GraphPad Prism 6.0 software. Determination of statistical significance between two comparisons was achieved using an unpaired *t* test. Determination of statistical significance between multiple comparisons was achieved using a one-way analysis of variance (ANOVA) followed by Dunnett's test with the appropriate controls. Normal distribution and equal variance between test groups were assumed prior to performing statistical tests using Prism software.

SUPPLEMENTAL MATERIAL

Supplemental material for this article may be found at https://doi.org/10.1128/AEM.00340-19.

SUPPLEMENTAL FILE 1, PDF file, 0.6 MB.

ACKNOWLEDGMENTS

We thank Bryon Donahoe for providing fluorescence micrographs and Ellsbeth Webb for technical assistance.

This work was conducted at the National Renewable Energy Laboratory (NREL), operated by the Alliance for Sustainable Energy, LLC, for the U.S. Department of Energy (DOE) under contract no. DE-AC36-08GO28308.

The work was supported in part by the Laboratory Directed Research and Development (LDRD) and Director's Fellowship Programs at NREL.

The views expressed in the article do not necessarily represent the views of the DOE or the U.S. Government.

REFERENCES

1. Garneau JE, Dupuis M-È, Villion M, Romero DA, Barrangou R, Boyaval P, Fremaux C, Horvath P, Magadán AH, Moineau S. 2010. The CRISPR/Cas bacterial immune system cleaves bacteriophage and plasmid DNA. Nature 468:67. https://doi.org/10.1038/nature09523.
2. Gasiunas G, Barrangou R, Horvath P, Siksnys V. 2012. Cas9-crRNA ribonucleoprotein complex mediates specific DNA cleavage for adaptive immunity in bacteria. Proc Natl Acad Sci U S A 109:E2579–E2586. https://doi.org/10.1073/pnas.1208507109.
3. Jinek M, Chylinski K, Fonfara I, Hauer M, Doudna JA, Charpentier E. 2012. A programmable dual-RNA-guided DNA endonuclease in adaptive bacterial immunity. Science 337:816–821. https://doi.org/10.1126/science.1225829.
4. Makarova KS, Grishin NV, Shabalina SA, Wolf YI, Koonin EV. 2006. A putative RNA-interference-based immune system in prokaryotes: computational analysis of the predicted enzymatic machinery, functional analogies with eukaryotic RNAi, and hypothetical mechanisms of action. Biol Direct 1:7. https://doi.org/10.1186/1745-6150-1-7.
5. Cui L, Bikard D. 2016. Consequences of Cas9 cleavage in the chromosome of Escherichia coli. Nucleic Acids Res 44:4243–4251. https://doi.org/10.1093/nar/gkw223.
6. Gupta R, Barkan D, Redelman-Sidi G, Shuman S, Glickman MS. 2011. Mycobacteria exploit three genetically distinct DNA double-strand break repair pathways. Mol Microbiol 79:316–330. https://doi.org/10.1111/j.1365-2958.2010.07463.x.
7. Xu T, Li Y, Shi Z, Hemme CL, Li Y, Zhu Y, Van Nostrand JD, He Z, Zhou J. 2015. Efficient genome editing in Clostridium cellulolyticum via CRISPR-Cas9 nickase. Appl Environ Microbiol 81:4423–4431. https://doi.org/10.1128/AEM.00873-15.
8. Li K, Cai D, Wang Z, He Z, Chen S. 2018. Development of an efficient genome editing tool in Bacillus licheniformis using CRISPR-Cas9 nickase. Appl Environ Microbiol 84:e02608-17. https://doi.org/10.1128/AEM.02608-17.
9. Song X, Huang H, Xiong Z, Ai L, Yang S. 2017. CRISPR-Cas9^{D10A} nickase-assisted genome editing in Lactobacillus casei. Appl Environ Microbiol 83:e01259-17. https://doi.org/10.1128/AEM.01259-17.
10. Garst AD, Bassalo MC, Pines G, Lynch SA, Halweg-Edwards AL, Liu R, Liang L, Wang Z, Zeitoun R, Alexander WG, Gill RT. 2017. Genome-wide mapping of mutations at single-nucleotide resolution for protein, metabolic and genome engineering. Nat Biotechnol 35:48. https://doi.org/10.1038/nbt.3718.
11. Li Y, Lin Z, Huang C, Zhang Y, Wang Z, Tang Y-J, Chen T, Zhao X. 2015. Metabolic engineering of Escherichia coli using CRISPR-Cas9 meditated genome editing. Metab Eng 31:13–21. https://doi.org/10.1016/j.ymben.2015.06.006.
12. Liang L, Liu R, Garst AD, Lee T, Nogué VSi, Beckham GT, Gill RT. 2017. CRISPR EnAbled Trackable genome Engineering for isopropanol production in Escherichia coli. Metab Eng 41:1–10. https://doi.org/10.1016/j.ymben.2017.02.009.
13. Hanson RS, Hanson TE. 1996. Methanotrophic bacteria. Microbiol Rev 60:439–471.
14. Ali H, Murrell JC. 2009. Development and validation of promoter-probe vectors for the study of methane monooxygenase gene expression in Methylococcus capsulatus Bath. Microbiology 155:761–771. https://doi.org/10.1099/mic.0.021816-0.
15. Csaki R, Bodrossy L, Klem J, Murrell JC, Kovacs KL. 2003. Genes involved in the copper-dependent regulation of soluble methane monooxygenase of Methylococcus capsulatus (Bath): cloning, sequencing and mutational analysis. Microbiology 149:1785–1795. https://doi.org/10.1099/mic.0.26061-0.
16. Welander PV, Summons RE. 2012. Discovery, taxonomic distribution, and phenotypic characterization of a gene required for 3-methylhopanoid production. Proc Natl Acad Sci U S A 109:12905–12910. https://doi.org/10.1073/pnas.1208255109.
17. Ishikawa M, Yokoe S, Kato S, Hori K. 2018. Efficient counterselection for Methylococcus capsulatus (Bath) by using a mutated pheS gene. Appl Environ Microbiol 84:e01875-18. https://doi.org/10.1128/AEM.01875-18.
18. Stolyar S, Costello AM, Peeples TL, Lidstrom ME. 1999. Role of multiple gene copies in particulate methane monooxygenase activity in the methane-oxidizing bacterium Methylococcus capsulatus Bath. Microbiology 145:1235–1244. https://doi.org/10.1099/13500872-145-5-1235.
19. Stolyar S, Franke M, Lidstrom ME. 2001. Expression of individual copies of Methylococcus capsulatus bath particulate methane monooxygenase genes. J Bacteriol 183:1810. https://doi.org/10.1128/JB.183.5.1810-1812.2001.
20. Henard CA, Guarnieri MT. 2018. Metabolic engineering of methanotrophic bacteria for industrial biomanufacturing, p 117–132. *In* Kalyuzhnaya MG, Xing X-H (ed), Methane biocatalysis: paving the way to sustainability. Springer International Publishing, New York, NY.
21. Henard CA, Smith H, Dowe N, Kalyuzhnaya MG, Pienkos PT, Guarnieri MT. 2016. Bioconversion of methane to lactate by an obligate methanotrophic bacterium. Sci Rep 6:21585. https://doi.org/10.1038/srep21585.
22. Nguyen AD, Hwang IY, Lee OK, Kim D, Kalyuzhnaya MG, Mariyana R, Hadiyati S, Kim MS, Lee EY. 2018. Systematic metabolic engineering of Methylomicrobium alcaliphilum 20Z for 2,3-butanediol production from methane. Metab Eng 47:323–333. https://doi.org/10.1016/j.ymben.2018.04.010.
23. Garg S, Clomburg JM, Gonzalez R. 2018. A modular approach for high-flux lactic acid production from methane in an industrial medium using engineered Methylomicrobium buryatense 5GB1. J Ind Microbiol Biotechnol 45:379–391. https://doi.org/10.1007/s10295-018-2035-3.
24. Garg S, Wu H, Clomburg JM, Bennett GN. 2018. Bioconversion of methane to C-4 carboxylic acids using carbon flux through acetyl-CoA in engineered Methylomicrobium buryatense 5GB1C. Metab Eng 48:175–183. https://doi.org/10.1016/j.ymben.2018.06.001.
25. Puri AW, Owen S, Chu F, Chavkin T, Beck DAC, Kalyuzhnaya MG, Lidstrom ME. 2015. Genetic tools for the industrially promising methanotroph Methylomicrobium buryatense. Appl Environ Microbiol 81:1775. https://doi.org/10.1128/AEM.03795-14.
26. Pédelacq J-D, Cabantous S, Tran T, Terwilliger TC, Waldo GS. 2006. Engineering and characterization of a superfolder green fluorescent protein. Nat Biotechnol 24:79. https://doi.org/10.1038/nbt1172.
27. Larsen Ø, Karlsen OA. 2016. Transcriptomic profiling of Methylococcus capsulatus (Bath) during growth with two different methane monooxygenases. Microbiologyopen 5:254–267. https://doi.org/10.1002/mbo3.324.
28. Nielsen AK, Gerdes K, Murrell JC. 1997. Copper-dependent reciprocal transcriptional regulation of methane monooxygenase genes in Methylococcus capsulatus and Methylosinus trichosporium. Mol Microbiol 25:399–409. https://doi.org/10.1046/j.1365-2958.1997.4801846.x.
29. Jiang W, Bikard D, Cox D, Zhang F, Marraffini LA. 2013. RNA-guided editing of bacterial genomes using CRISPR-Cas systems. Nat Biotechnol 31:233–239. https://doi.org/10.1038/nbt.2508.
30. Glaser A, McColl B, Vadolas J. 2016. GFP to BFP conversion: a versatile assay for the quantification of CRISPR/Cas9-mediated genome editing. Mol Ther Nucleic Acids 5:e334. https://doi.org/10.1038/mtna.2016.48.
31. Metzger MJ, McConnell-Smith A, Stoddard BL, Miller AD. 2011. Single-strand nicks induce homologous recombination with less toxicity than double-strand breaks using an AAV vector template. Nucleic Acids Res 39:926–935. https://doi.org/10.1093/nar/gkq826.
32. Bassalo MC, Garst AD, Halweg-Edwards AL, Grau WC, Domaille DW, Mutalik VK, Arkin AP, Gill RT. 2016. Rapid and efficient one-step metabolic pathway integration in E. coli. ACS Synth Biol 5:561–568. https://doi.org/10.1021/acssynbio.5b00187.
33. Corts AD, Thomason LC, Gill RT, Gralnick JA. 2019. A new recombineering system for precise genome-editing in Shewanella oneidensis strain MR-1 using single-stranded oligonucleotides. Sci Rep 9:39. https://doi.org/10.1038/s41598-018-37025-4.
34. Slaymaker IM, Gao L, Zetsche B, Scott DA, Yan WX, Zhang F. 2016. Rationally engineered Cas9 nucleases with improved specificity. Science 351:84–88. https://doi.org/10.1126/science.aad5227.
35. Chen JS, Dagdas YS, Kleinstiver BP, Welch MM, Sousa AA, Harrington LB, Sternberg SH, Joung JK, Yildiz A, Doudna JA. 2017. Enhanced proofreading governs CRISPR-Cas9 targeting accuracy. Nature 550:407–410. https://doi.org/10.1038/nature24268.
36. Hu JH, Miller SM, Geurts MH, Tang W, Chen L, Sun N, Zeina CM, Gao X, Rees HA, Lin Z, Liu DR. 2018. Evolved Cas9 variants with broad PAM compatibility and high DNA specificity. Nature 556:57–63. https://doi.org/10.1038/nature26155.
37. Kleinstiver BP, Pattanayak V, Prew MS, Tsai SQ, Nguyen NT, Zheng Z, Joung JK. 2016. High-fidelity CRISPR-Cas9 nucleases with no detectable

genome-wide off-target effects. Nature 529:490–495. https://doi.org/10.1038/nature16526.
38. Qi LS, Larson MH, Gilbert LA, Doudna JA, Weissman JS, Arkin AP, Lim WA. 2013. Repurposing CRISPR as an RNA-guided platform for sequence-specific control of gene expression. Cell 152:1173–1183. https://doi.org/10.1016/j.cell.2013.02.022.
39. Gaudelli NM, Komor AC, Rees HA, Packer MS, Badran AH, Bryson DI, Liu DR. 2017. Programmable base editing of A*T to G*C in genomic DNA without DNA cleavage. Nature 551:464–471. https://doi.org/10.1038/nature24644.
40. Guilinger JP, Thompson DB, Liu DR. 2014. Fusion of catalytically inactive Cas9 to FokI nuclease improves the specificity of genome modification. Nat Biotechnol 32:577–582. https://doi.org/10.1038/nbt.2909.
41. Komor AC, Kim YB, Packer MS, Zuris JA, Liu DR. 2016. Programmable editing of a target base in genomic DNA without double-stranded DNA cleavage. Nature 533:420–424. https://doi.org/10.1038/nature17946.
42. Whittenbury R, Phillips KC, Wilkinson JF. 1970. Enrichment, isolation and some properties of methane-utilizing bacteria. Microbiology 61:205–218. https://doi.org/10.1099/00221287-61-2-205.
43. Graham DW, Korich DG, LeBlanc RP, Sinclair NA, Arnold RG. 1992. Applications of a colorimetric plate assay for soluble methane monooxygenase activity. Appl Environ Microbiol 58:2231–2236.
44. Guerry P, van Embden J, Falkow S. 1974. Molecular nature of two nonconjugative plasmids carrying drug resistance genes. J Bacteriol 117:619–630.
45. Kovach ME, Elzer PH, Hill DS, Robertson GT, Farris MA, Roop RM, Peterson KM. 1995. Four new derivatives of the broad-host-range cloning vector pBBR1MCS, carrying different antibiotic-resistance cassettes. Gene 166:175–176. https://doi.org/10.1016/0378-1119(95)00584-1.